

# ENHANCING THE HARMONIC CONTENT OF AN HGHG MICROBUNCH

Kirsten Hacker, TU, Dortmund, Germany

## Abstract

High Gain Harmonic Generation (HGHG) seeding has been demonstrated in the visible and ultraviolet, but it is limited in performance at high harmonics of the seed by the initial uncorrelated energy spread of the electron beam. A recent proposal from SINAP using a chirped electron beam and a canted pole undulator has suggested a new mechanism for reducing the length of the seeded microbunches in order to improve the performance of HGHG seeding at high harmonics. This note reviews the mechanism, the limitation of the concept and extrapolates to some new concepts using analogous mechanisms derived from transverse gradients of the laser properties. The impact of CSR wakes on the vanishingly short microbunches produced by the methods are also investigated.

## INTRODUCTION

Seeded electron beams benefit from a small uncorrelated energy spread of the electron beam because it reduces the length of the seeded microbunches. For High Gain Harmonic Generation (HGHG) seeding, the bunching factor as a function of harmonic number  $n$  is given in terms of the uncorrelated energy spread,  $\delta$ , by [1]

$$b_n = e^{-(nD\delta)^2/2} J_n(nD\Delta\gamma) \quad (1)$$

where  $\Delta\gamma$  is the energy modulation,  $n$  is the harmonic number,  $D=2\pi R_{56}/\lambda_s\gamma_0$  where  $R_{56}$  is the dispersion of the chicane and  $J_n$  is a Bessel function of order  $n$ . When the bunching factor is plotted for a range of slice energy spreads, it is apparent that the seeding method could be extended to shorter wavelengths if a technique could reduce or cool the slice energy spread,  $\delta$ , prior to or during seeding (Fig. 1).

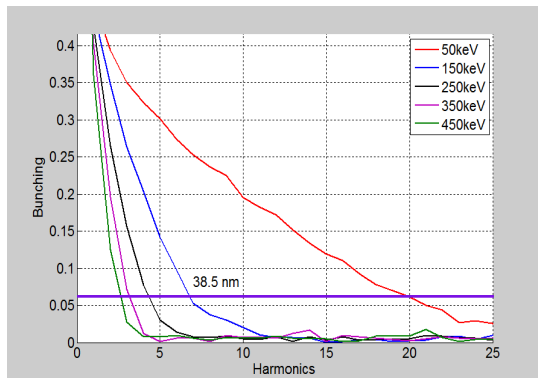


Figure 1: Bunching factor as a function of harmonics for a range of initial uncorrelated energy spreads for a 270 nm HGHG seeded beam.

\*work supported by BMBF grant 05K10PE1 and DESY.

Several ideas have been proposed to cool the slice energy spread of an electron beam prior to seeding. The least invasive strategy involves reducing the compression and charge of the electron bunch so that it is easier to transport without suffering from the nonlinearities introduced by various wakefields which scale with the peak current. In simulations, this alone is enough to achieve a 100 keV slice energy spread at FLASH2 [2]. In practice, this is less certain. This strategy also reduces the FEL peak power, since the peak power scales with the peak current.

The next strategy employs a laser heater in the first bunch compressor of the accelerator in order to increase (heat) the uncorrelated energy spread early in the machine and smear out random fine structures in the electron bunch which get amplified as they propagate over large distances [3,4]. The combination of low-charge, weak compression, and laser heating has been shown to reduce the slice energy spread of the Elettra at FERMI beam to ~150 keV for a 500 nC bunch with 500 A of peak current prior to the seeding section [4].

An untried strategy from SINAP uses a canted pole undulator with a transversely chirped electron bunch in order to reduce the effective length of HGHG microbunches [1]. In this note, simulation predictions from seeding with SINAP's canted pole undulator are duplicated and extrapolated to alternatives utilizing novel laser conditions like a transverse intensity gradient, a wavefront rotation, and a transverse chirp as an alternative to the canted undulator pole. The benefits and problems associated with these alternatives are described.

## CANTED POLE SEEDING

The SINAP HGHG proposal is to send a transversely chirped electron bunch through an undulator with transversely canted poles (Fig. 2).

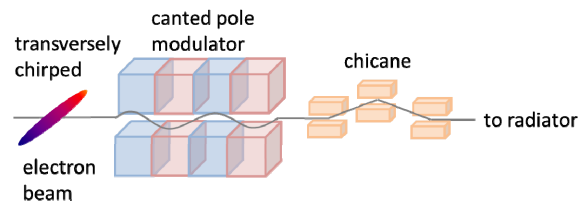


Figure 2: SINAP HGHG proposal sends a transversely chirped electron bunch through an undulator with transversely canted poles.

The mechanism was described by SINAP in the language of off-resonance seed laser modulation for cooling the beam energy spread. This note investigates the mechanism in the language of path length changes and energy transfer from the laser to the electron beam. It then extrapolates to scenarios with transverse variations of

laser properties in place of a transverse undulator gradient.

The longitudinal displacement of an electron traveling through an undulator magnet is given by [4]

$$z(t) = \bar{v}_z t - \frac{cK^2}{8\gamma^2\omega_u} \sin(2\omega_u t), \quad (2)$$

where

$$\bar{v}_z = 1 - \frac{1}{2\gamma^2} \left( 1 + \frac{K^2}{2} \right). \quad (3)$$

Substitute in the time-of-flight through the modulator,  $\Delta t = N\lambda_u/c$  and the angular frequency  $\omega_u = 2\pi/\lambda_u$  to get

$$z(\Delta t) = \frac{\bar{v}_z N\lambda_u}{c} - \frac{c\lambda_u K^2}{16\gamma^2\pi} \sin(4\pi N/c).$$

Now, substituting in the  $x$  dependent portion of  $v_z$  and writing  $z(x)$  for the canted poles and transversely chirped electron beam gives

$$z(x) = \frac{K(x)^2 N\lambda_u}{4\gamma(x)^2 c} - \frac{c\lambda_u K(x)^2}{16\gamma(x)^2 \pi} \sin(4\pi N/c).$$

Separating out the  $x$  dependent terms and writing the longitudinal coordinate for the left and right sides of the beam gives

$$z(x_{left}) = \frac{K(x_{left})^2}{\gamma(x_{left})^2} \left( \frac{N\lambda_u}{4c} - \frac{c\lambda_u \sin(4\pi N/c)}{16\pi} \right)$$

$$z(x_{right}) = \frac{K(x_{right})^2}{\gamma(x_{right})^2} \left( \frac{N\lambda_u}{4c} - \frac{c\lambda_u \sin(4\pi N/c)}{16\pi} \right).$$

Let us call the constant on the right,  $C$ , so that the difference in the longitudinal position across the transversely chirped electron bunch in the canted undulator pole is written

$$\Delta z = C \left( \frac{K_{left}^2}{\gamma_{left}^2} - \frac{K_{right}^2}{\gamma_{right}^2} \right) \quad (4)$$

If  $\Delta z$  goes to zero, the microbunch still has a length determined by the uncorrelated energy spread. This microbunch length can be written in terms of the transfer matrix element for dispersion as

$$\Delta z = R_{56} \frac{\Delta E}{E}, \quad (5)$$

where the  $R_{56}$  of an undulator is [5,6]

ISBN 978-3-95450-133-5

$$R_{56} = \frac{N\lambda_u}{\gamma_0^2} \left( 1 + \frac{3K^2}{2} \right). \quad (6)$$

Equating Eq. 3 and 4 gives the condition for a minimum microbunch length.

The entire energy modulated waveform on the right side of the electron bunch starts out earlier and arrives later than the entire waveform on the left and this happens for a special combination of  $\gamma$  and  $K$  which is given in terms of the resonance condition by Eq. 6 of SINAP's paper [7] and, equivalently, in terms of path lengths, by Eq. 3 and 4, above.

Using the SINAP conditions as an example, Eq. 3 and 4 can be used to reproduce the phenomenon in simulation. The beam energy was 0.84 GeV with 84 keV (rms) slice energy spread (0.01%), 600 A peak current, modulator period length of 80 mm, and period number of 12. The induced energy modulation was 500 keV with a 265 nm seed. These conditions can be replicated in a simulation with a beam made up of two stripes of different energies which differ from the reference energy by 0.01%. In Fig. 3, the beam is given an energy modulation and is bunched through the  $R_{56}$  term alone.

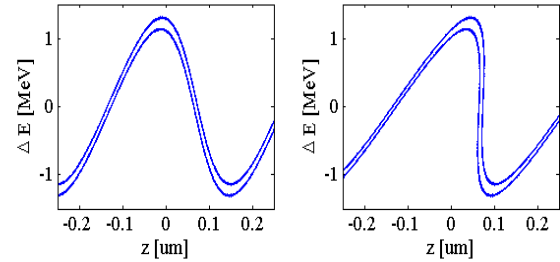


Figure 3: Stripes of charge with different energies in longitudinal phase space modulated with a sinusoidal pattern and then bunched in a chicane.

By varying  $K$  by  $\pm 0.07\%$  in Eq. 3, the SINAP results are reproduced as shown in Fig. 4.

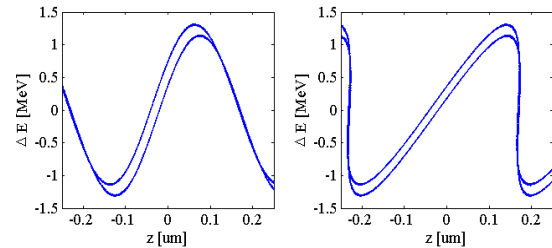


Figure 4: Eq. 4 reproduces the SINAP result with the canted pole undulator and transversely chirped electron bunch.

The same effect can be generated by shifting one curve longitudinally by 10 nm according to  $R_{51} \Delta x = 10$  nm. While the  $R_{56}$  does vary transversely across the transversely chirped bunch, the effect is negligible compared to the non-energy-dependent path length changes from the  $R_{51}$ .

The magnetic field tolerances of the method depend on the energy spread and dispersion of the electron bunch. For the SINAP example, where the K needs to vary by  $\pm 0.07\%$ , a gap,  $g=10$  mm, would need to vary by  $13 \mu\text{m}$  over  $2\sigma$  of the electron beam according to Eq. 63 of [7],

$$\frac{dg}{dx} \Delta x = -\frac{\Delta K}{K} \frac{\lambda_u}{\pi} \coth^{-1}(\pi g / \lambda_u).$$

Another important tolerance evolves around coherent synchrotron radiation (CSR) and longitudinal space charge (LSC). The compression in the above simulations was done in 1-D through  $R_{56}$  alone and does not take into account the impact of CSR and LSC. The high peak currents of vanishingly short microbunches can dramatically increase the energy spread and influence the charge distribution after a chicane and a drift [8] and increasing the peak current by shortening the length of the microbunch with this canted pole method could, therefore, be counterproductive. Compression through a drift alone would avoid the CSR and might provide a preferable mode of compression [8]. The drawback of producing a spatially chirped FEL beam should also be considered.

### LASER COOLED SEEDING

An alternative to the canted pole technique exploits an analogous mechanism with laser techniques. Tolerances for these techniques are described.

In the case of a tilted laser wavefront produced by giving the trajectory of the laser pulse through the modulator an angle, the condition plotted in Fig. 4 could theoretically be reproduced using the laser wavefront rotation in lieu of the canted undulator pole. The wavefront rotation method would offer superior tunability compared to the canted pole undulator method at a cost of increased sensitivity to a coupled, unstable, and difficult to measure laser parameter (Fig. 5).

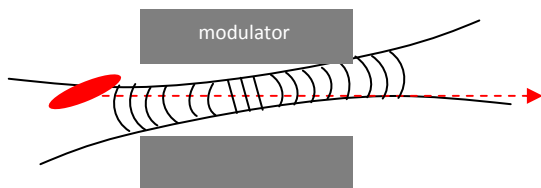


Figure 5: Wavefront rotation due to diagonal trajectory through the modulator. The dashed line is the trajectory of the electrons while the solid lines represent the laser waist and wavefronts. If the waist of the seed is too small, curvature of the wavefronts can complicate the technique along with coupling between modulation amplitude and trajectory.

The wavefront angle required by such a technique is determined by the energy spread which requires correction. If the 84 keV slice energy spread from the SINAP example is used, the laser wavefront would need to arrive 10 nm earlier on the left compared to the right.

For an electron beam which is dispersed by 1 mm at the entrance to the modulator, this corresponds to an angle of  $10 \mu\text{rad}$  of the laser wavefront with respect to the electron beam trajectory. Pointing jitter of an injected beam after 20 meters of transport would be on this level, but fast steering correction systems are technically possible. With more electron beam dispersion or slice energy spread, the tolerances on the laser pointing jitter are relaxed. For example, at DELTA, the electron beam could be streaked by 1 cm and require  $100 \mu\text{rad}$  of wavefront rotation to demonstrate the effect [9].

Since the transverse overlap in the modulator is coupled to the seed trajectory, this technique can be complicated by coupling between energy modulation amplitude and wavefront tilt. Especially for longer, 2 meter modulators, it could be difficult to distinguish which change in the harmonic content is due to the wavefront rotation change and which is due to the modulation amplitude. However, when the seed spot diameter is a few times larger than that of the electron beam, this coupling effect is tiny.

An alternative way to apply tilted wavefronts is to place the modulator off-center with respect to the laser waist and then misalign the seed pulse compressor so that a wavefront rotation is produced in the modulator (Fig. 6). Compressor misalignments would change the steering into the modulator unless a steering feedback is used to correct the orbit, but there are commercial systems which can do this. Away from the waist, the wavefront rotation disappears and becomes a pulse-front tilt (variation in the arrival time of the intensity fronts), but on-average, the wavefront would be rotated in a single direction and it could be tuned without impacting the overlap. The pulse length, however would be sensitive to large changes in compressor alignment. If the compressor alignment changes are small, then the impact of pulse length changes on the energy modulation should be small.

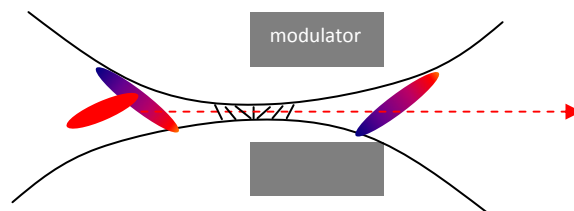


Figure 6: Wavefront rotation produced through compressor misalignment. The pulse has wavefront rotation at the waist and pulse front tilt away from the waist. It has spatial chirp throughout. The dashed line is the trajectory of the electrons while the solid lines represent the laser waist and wavefront rotation.

The impact of the spatial chirp which accompanies the compressor misalignment could be significant (Fig. 6). To remove the effect of an 85 keV electron bunch slice energy spread with a spatially chirped laser pulse, the laser would need to be chirped from 395 nm on one side to 405 nm on the other. This is possible with the bandwidth of the current sFLASH laser system and the

sFLASH modulators, however, to correct for a larger, 400 keV energy spread, a 40 nm bandwidth of a 270 nm seed would be required. This verges on the impossible with known techniques. A spatially chirped laser pulse would necessarily have a significant pulse front tilt and the waist would need to be placed away from the modulator in order to avoid the influence of wavefront rotation which occurs near the waist. The pulse front tilt would also complicate longitudinal overlap with the electron bunch since the electron bunch would need to be chirped in the same plane as the pulse front tilt (Fig. 7).

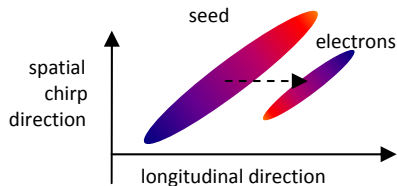


Figure 7: Longitudinal and spatial overlap of chirped electron and chirped seed. Since the seed must be larger than the electron bunch to ensure a flat intensity profile, this method presents challenging overlap and bandwidth considerations.

With an offset from the center of the laser spot, the electron beam will see a slightly tilted wavefront and an intensity gradient (Fig. 8). For large laser spots, the intensity gradient would be the dominant effect and could be used to cool the energy spread.

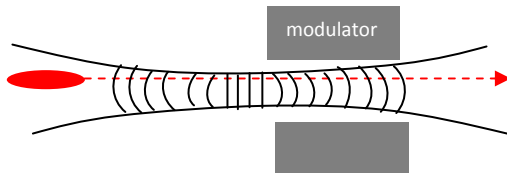


Figure 8: Transverse intensity gradient and wavefront rotation due to offset relative to center of laser spot.

Compared to the wavefront rotation, the intensity gradient is the dominant effect whenever the electron beam is off center from the laser spot and when the compressor is not misaligned. The effect of this intensity gradient on the longitudinal phase space is shown below in Fig. 9. The two particle trajectories come closer together for negative energies but grow further apart for positive energies. The area between the two curves remains constant, per Liouville's theorem.

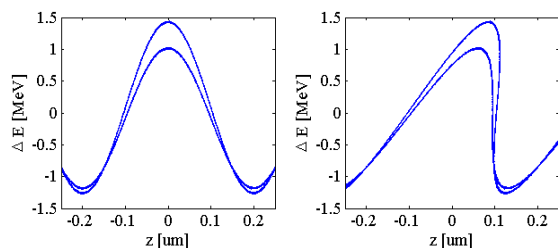


Figure 9: The effect of a transverse laser intensity gradient which transversely varies the energy transferred from the seed to the transversely chirped electron bunch.

The tolerances of such a technique would require a precise laser intensity gradient to be matched to a precise electron beam energy chirp. While tuning the slope of the laser gradient by increasing and decreasing the laser pulse energy could be simple, the energy modulation would also increase and decrease, complicating the method.

A beneficial operation point is found when the transverse gradient technique is combined with a CSR wake from the last dipole of the bunching chicane. While a symmetrically compressed bunch would become chirped by the CSR wake, so that low energy particles get bunched more than the high energy particles, if this is combined with the transverse laser gradient technique and a slightly over compressed bunch, a more dramatic spike in the peak current could be achieved.

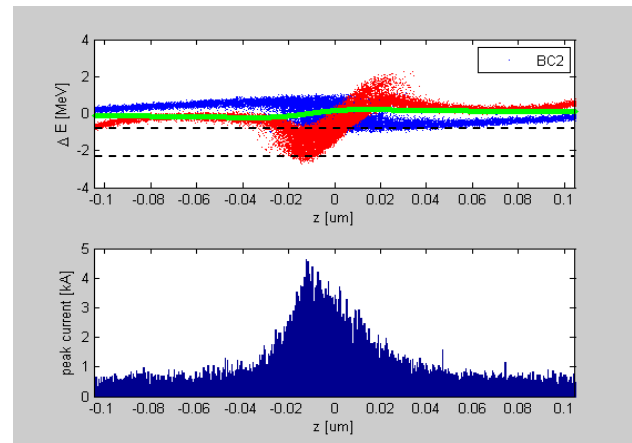


Figure 10: Impact of LSC and CSR on a microbunch after 4 meters of drift and an  $R_{56}$  of 45  $\mu\text{m}$ . Dashed lines represent the bandwidth of the radiator. The background particles in blue show the conditions prior to the application of CSR or LSC. The foreground, red particles show the bunch after CSR and LSC and 4 meters of drift. The green line gives the LSC potential per meter. This is done for a 700 MeV beam energy, 1 kA initial peak current, and 2 MeV (pp) energy modulation. The harmonic content of the microbunch was unaffected, but the energy spread was increased.

## CONCLUSION

The canted pole undulator technique has tight tolerances on the gap and tunability. Alternatives which combine a dispersed electron bunch with different laser properties in the modulator could be used to produce a similar effect with more tunability, however, each alternative introduces undesirable byproducts in terms of coupled parameters and sensitivity to unstable laser parameters. The most promising technique appears to be to use a transverse laser intensity gradient with a transversely chirped electron bunch. It has reasonable tolerances and provides a mechanism for increasing the microbunch peak current by making use of a CSR wake. For the other methods, CSR destroys the quality of the microbunch, but for the transverse intensity gradient, it enhances it.

**REFERENCES**

- [1] H. Deng and C. Feng, PRL 111, 084801 (2013).
- [2] G. Feng, et al., These Proceedings: Proc. 36th Int. Free-Electron Laser Conf., Basel, 2014, MOP083.
- [3] Z. Huang, et al., PRST-AB 13, 020703 (2010).
- [4] E. Allaria et al., Nat. Photonics 7, 913 (2013).
- [5] P. Schmueser, et al., Springer (2008).
- [6] Y. Li and J. Pflueger, Proc. FEL 2010, 37 (2010).
- [7] Z. Wolf, "Algorithms To Automate LCLS Undulator Tuning" April 10, 2006, LCLS-TN-06-8, page 26.
- [8] K. Hacker, These Proceedings: Proc. 36th Int. Free-Electron Laser Conf., Basel, 2014, MOP095.
- [9] S. Khan, These Proceedings: Proc. 36th Int. Free-Electron Laser Conf., Basel, 2014, MOP084.